Laser Photolysis of Matrix-Isolated Methyl Nitrate: Experimental and Theoretical Characterization of the Infrared Spectrum of Imine Peroxide (HNOO)

Ping Ling, Alexander I. Boldyrev, Jack Simons, and Charles A. Wight*

Contribution from the Department of Chemistry, University of Utah, Salt Lake City, Utah 84112-0850

Received July 9, 1998

Abstract: Photodissociation of methyl nitrate (and its fully deuterated isotopomer) isolated in an argon matrix at 17 K has been investigated by 266 nm laser photolysis. Characterization of the product species has been performed by transmission Fourier transform infrared spectroscopy. There are two parallel initial reaction channels, one of which is formation of formaldehyde (H_2CO) and hydrogen nitryl (HNO_2). The second channel is formation of formaldehyde and a previously unreported species, imine peroxide (HNOO). Quantum chemical calculations of the structure, vibrational frequencies, and infrared band intensities have been performed at the B3LYP/6-311++G**, MP2(full)/6-311++G**, and QCISD/6-311++** levels of theory. The calculated vibrational frequency patterns allowed us to confirm the detection and infrared spectral assignments of imine peroxide for the first time.

Introduction

Because of their high oxygen content, nitrate esters of organic compounds have been widely used as energetic materials. The mechanism of thermal decomposition on the ground electronic manifold of states has been previously investigated for several different types of nitrate esters.[1−3] However, little is known about their photodissociation pathways from electronically excited states. This subject is of current interest for energetic materials because it has been postulated that electronic excitation and predissociation of energetic materials may be important in the chemical mechanism of initiation and propagation of detonation shock waves.[4−7] As more is learned about the complex chemical and physical mechanisms of detonation, through experimental studies and molecular dynamics calculations,[8] the possible role of electronically excited states in the process is expected to become clarified.

Recently, we reported an experimental study which revealed that thermal and photochemical decompositions of poly(glycidyl nitrate), or PGN, occur by distinctly different pathways.[9] PGN is a technologically important material that is used as an energetic polymer binder in solid rocket propellant formulations. However, the material and its chemistry are both quite complex, involving formation of mixtures of several products that are difficult to identify in the condensed phase. We therefore initiated the current study in order to investigate the photochemistry of the simplest organic nitrate ester, methyl nitrate, at a high level of detail.

Although there have been many previously reported studies of the photochemistry of organic and inorganic nitro compounds, nitroso compounds, and nitrites,[10−14] we were unable to find any studies of product branching or photochemical quantum yields for nitrate esters. This is despite a growing interest in the role of photochemistry of organic nitrate salts in atmospheric chemistry.[15,16] Clark and Hester[12] have reviewed much of the literature on matrix isolation spectroscopic studies of nitrogen-containing organic compounds, but nitrate esters were not mentioned. We chose the rare gas matrix isolation technique to study methyl nitrate because it provides a means of generating and preserving sufficiently high concentrations of reactive chemical intermediates for spectroscopic identification and characterization. In fact, the photochemistry of nitromethane was one of the pioneering works in the matrix isolation field and was the first to experimentally identify the existence of HNO. Since then, numerous species have been identified using this technique. The objective of this paper is to report the photochemistry of methyl nitrate isolated at low concentrations in an argon matrix at 17 K. On the basis of an identification of the reaction products and an analysis of their kinetic behavior, we were able to determine the major initial photodissociation channels under these experimental conditions.

* To whom correspondence should be addressed. E-mail: wight@chemistry.chem.utah.edu.

(1) Waring, C. E.; Krastine, G. *J. Phys. Chem.* **1970**, *74*, 999.
(2) Hiskey, M. A.; Brower, K. R.; Oxley, J. C. *J. Phys. Chem.* **1991**, *95*, 3955.
(3) Chen, J. K.; Brill, T. B. *Combust. Flame* **1991**, *85*, 479.
(4) Odiot, S. In *Chemistry and Physics of Energetic Materials*; Bulusu, S. N., Ed.; Kluwer Academic Publishers: Dordrecht, The Nertherlands, 1990; p 79.
(5) Kunz, A. B. *Phys. Rev. B* **1996**, *53*, 9733.
(6) Rice, B. M.; Mattson, W.; Grosh, J.; Trevino, S. F. *Phys. Rev. E* **1996**, *53*, 611.
(7) Aduev, B. P.; Aluker, E. D.; Krechetov, A. G. *Tech. Phys. Lett.* **1996**, *22*, 236.
(8) 8 Elert, M. L.; Deaven, D. M.; Brenner, D. W.; White, C. T. *Phys. Rev. B* **1989**, *39*, 1453.
(9) Ling, P.; Wight, C. A. *J. Phys. Chem. B* **1997**, *101*, 2126.
(10) Brown, H. W.; Pimentel, G. C. *J. Chem. Phys.* **1958**, *29*, 883.
(11) Muller, R. P.; Russegger, P.; Huber, J. R. *Chem. Phys.* **1982**, *70*, 281.
(12) Clark, R. J. H.; Hester, R. E. In *Spectroscopy of Matrix Isolated Species*; John Wiley & Sons Ltd.: New York, 1989; pp 190−422 and many references cited therein.
(13) Cheng, B. M.; Lee, J. W.; Lee, Y. P. *J. Phys. Chem.* **1991**, *95*, 2814.
(14) Hjorth, J.; Ottobrini, G.; Restell, G. *J. Phys. Chem.* **1988**, *92*, 2669.
(15) Calvert, J. G.; Pitts, J. N., Jr. In *Photochemistry*; John Wiley: New York, 1966; p 480.
(16) Barners, I.; Becker, K. H.; Starcke, J. *J. Phys. Chem.* **1991**, *95*, 9736.

10.1021/ja9824223 CCC: $15.00
Published on Web 11/12/1998

Experimental Section

Methyl nitrate and its fully deuterated isotopomer were prepared by esterification of CH_3OH (CD_3OH) with nitric acid in the presence of sulfuric acid as described previously.[17] Argon matrix isolated methyl nitrate was prepared by deposition of premixed methyl nitrate vapor and argon gas onto a 17 K CsI window in a high-vacuum deposition chamber. The base pressure of this chamber was maintained at 10^{-7} Torr by a turbomolecular pump to avoid contamination of the samples by impurity gases. The CsI window was cooled by a closed-cycle helium refrigerator (CTI Cryogenics model 22), and the temperature was maintained by a Lakeshore Cryotronics model 320 temperature controller. Deposition rate was typically $\sim 10^{-5}$ (mol/cm^2)/min at the sample window. After deposition, the sample temperature was quickly raised to 30 K for about 1 min and then lowered to 17 K in order to anneal the argon matrix to minimize multiple-site occupation of the methyl nitrate molecules.

Methyl nitrate exhibits a weak n$-\pi^*$ absorption around 270 nm. The photolysis was performed by using the fourth harmonic of a Nd:YAG laser (Continuum model Surelite) at 266 nm. The pulse duration was 7 ns, and a lens was used to expand the beam to approximately 3.5 cm^2 such that the average laser intensity was 10 mW/cm^2 (at 10 Hz repetition rate) at the sample surface. The bulk temperature change of the sample by absorption of the laser beam was negligible (<1 K).

Transmission FTIR spectra were recorded before photolysis and at regular intervals during photolysis in order to monitor intensity changes of the reactant and product peaks. Each spectrum was obtained using a Mattson model RS/10000 FTIR spectrometer by averaging 32 scans at 0.25 cm^{-1} resolution.

Following the primary photolysis period at 266 nm, samples were subjected to additional photolysis periods at 355 or 532 nm (third and second harmonics of the same laser) in order to aid the identification of reaction products.

The absorption coefficient of neat liquid methyl nitrate at 266 nm was measured by a Hewlett-Packard UV−visible diode array spectrometer.

Experimental Results

Photolysis of matrix-isolated methyl nitrate was conducted using samples prepared at mole ratios in the range 1:1000 to 1:5000 (CH_3ONO_2:Ar). The IR spectra of matrix-isolated methyl nitrate and its normal-coordinate analysis have been studied by Lannon et al.[18] At this dilution, the guest molecules are well isolated and the concentration of dimers and higher oligomers is negligible. The IR spectra show that CH_3ONO_2 molecules occupy multiple sites in the argon matrix, as indicated by closely spaced multiple absorption peaks for many modes in the spectrum.

After 266 nm photolysis, numerous new bands appear. The spectra show that reaction products also occupy multiple sites in the argon lattice. The positions of these product bands of photolyzed CH_3ONO_2/Ar and CD_3ONO_2/Ar are listed in Tables 1 and 2, respectively. For simplicity, we have listed only the absorption bands of dominant sites; however, if absorption bands corresponding to two sites were comparable, we listed both.

To assign the new bands to corresponding products, we employed an approach based on three criteria:

(1) The growth in intensity of all peaks during 266 nm photolysis was analyzed to determine possible correlations in the band intensities and to determine whether each peak exhibits an induction period.

(2) After 266 nm photolysis for several hours, we used secondary photolysis periods at 355 and/or 532 nm to selectively destroy the reaction products. Because different products respond differently to these wavelengths, this technique aids in establishing correlations among the bands and assignments to the various products.

(3) We compared the band positions with literature values where available and otherwise with vibrational frequencies determined using ab initio quantum chemical calculations of suspected products. We performed experiments on two isotopomers of methyl nitrate, CH_3ONO_2 and CD_3ONO_2, to check the band assignments with the calculated values.

Tables 1 and 2 list the photolysis product infrared band intensities from CH_3ONO_2 and CD_3ONO_2 after 20 and 520 min exposure to 266 nm radiation. The relative intensity distributions of product bands of photolyzed CH_3ONO_2 are also shown in Figure 1. Note that the spectra of the initial products (after 20 min photolysis) are fairly simple compared with spectra recorded after a long periods of irradiation. The initial product bands, which are labeled A, B, or C, all exhibit the same qualitative behavior during 266 nm photolysis, as illustrated for three representative bands in Figure 2. Note that none of the bands of the initial products exhibit a noticeable induction period; that is, the bands have their maximum rate of growth at $t = 0$.

In contrast, several secondary photolysis products were observed, including H_2O, CO_2, CO, HNO, *cis*- and *trans*-

Table 1. Photoproduct Infrared Bands (CH_3ONO_2:Ar = 1:1500 at 266 nm)

wavenumber (cm^{-1})	rel intens[a] after 20 min photolysis		rel intens[a] after 520 min photolysis	possible product assignt
3712.9	0.054		2.51	H_2O
3622.4	0		0.17	O−H?
3616.1	0.033		0.14	O−H?
3608.3	0		1.06	H_2O
3498.7	0		0.94	HONO-*trans*
3360.1	0		0.56	HONO-*cis*
3287.7/3306	2.93	C	3.12	HNOO
3137.1	1.85	B	1.84	HNO_2
3049.4	0		0.43	HNO
2831.4	0.53	A	0.48	H_2CO
2822.7	0		0.13	C−H?
2731.3	0.079		0.10	C−H?
2715.1	0.068		0.14	C−H?
2344.5	0.042		3.13	CO_2
2151.9	0.057		2.81	CO
1876.4	0		0.35	NO
1762.4	0		0.33	HC(═O)OH
1747.8/1743.4	0		0.50	HC(═O)NO?
1725.8	1.00	A	1.00	H_2CO
1680.2	0		0.45	HONO-*trans*
1625.4	0		0.69	HONO-*cis*
1605.3/1603.2	0.71	B	0.66	HNO_2
1594.0/1591.4	0		1.13	HC(═O)NO?
1580.3/1575.5	0		1.32	HNO
1497.4	0		0.13	HNO
1493.4	0.23	A	0.24	H_2CO
1381.6	0.69	C	0.74	HNOO
1371.6	0.073	B	0.074	HNO_2
1310.3	0.055		0.34	HONO-*trans*
1252.2	0.066	A	0.072	H_2CO
1183.7	0.096		0.89	C−O?
1155.3	0.078		0.31	C−O?
1116.2	0		0.35	C−O?
923.6	1.37	B	1.42	HNO_2
843.2	0.38	C	0.35	HNOO
868.7	0		1.12	HONO-*cis*
837.5	0.22	B	0.24	HNO_2
813.2	0		0.62	HONO-*trans*
790.7	0.33	C	0.32	HNOO
670.1	0.19	C	0.19	HNOO
628.1	0		0.28	HONO-*trans*,*cis*?

[a] Normalized to the intensity of H_2CO at 1725.8 cm^{-1}.

(17) Johnson, J. R. In *Organic Syntheses*; John Wiley Ltd.: New York, 1939; Vol. XIX, p 64.

(18) Lannon, J. A.; Harris, L. E.; Verderame, F. D.; Thomas, W. G.; Lucia, E. A.; Koniers. S. *J. Mol. Spectrosc.* **1974**, *50*, 68.

Table 2. Photoproduct Infrared Bands (CD_3ONO_2:Ar = 1:1500 at 266 nm)

wavenumber (cm^{-1})	rel intens[a] after 40 min photolysis		rel intens[a] after 518 min photolysis	possible product assignt
2766.5	0		0.12	D−O?
2756.3	0.016		0.77	D_2O
2739.6	0		0.16	D−O?
2637.0	0		0.23	D_2O
2443.5	1.65	C	2.02	DNOO
2342.2	0.021		0.88	CO_2
2334.1	0		0.32	DONO-*trans*
2315.3	0.33	B	0.32	DNO_2
2259.4	0		0.16	DNO
2214.8	0		0.30	DONO-*cis*
2152.7	0.019		0.65	CO
2139.9	0		0.087	C−D?
2118.2	0		0.076	C−D?
2094.5	0.57	A	0.64	D_2CO
1875.7	0		0.068	NO
1719.0/1714.4	0		0.13	DC(=O)OD
1709.5/1705.5	0		0.14	DC(=O)NO?
1704.3/1700.1	0		0.28	DC(=O)NO?
1695.7	0		0.019	?
1679.9	1.00	A	1.00	D_2CO
1671.5	0		0.031	DONO-*trans*
1578.9/1575.8	0.53	B	0.61	DNO_2
1569.5/1566.6	0		0.022	DC(=O)NO?
1561.7/1558.4	0		0.078	DC(=O)NO?
1541.4	0		0.28	DNO
1196.4	0		0.11	C−O?
1179.3−1172.9	0.042		0.50	C−O?
1112.7	0.092	B	0.075	DNO_2
1081.1/1079.2	0.79	C	0.87	DNOO
1036.8	0		0.056	DONO-*trans*
992.1	0		0.12	DONO-*cis*?
971.3	0.014		0.10	?
895.5/892.2	0.97	B	1.22	DNO_2
834.3/832.2	0.11	B	0.095	DNO_2
823.4/822.0	0.24	C	0.33	DNOO
658.7	0.096	C	0.11	DNOO
636.3	0		0.28	DONO-*cis*
618.9	0		0.012	DONO-*trans*
588.1/585.7	0.33	C	0.29	DNOO

[a] Normalized to the intensity of D_2CO at 1679.9 cm^{-1}.

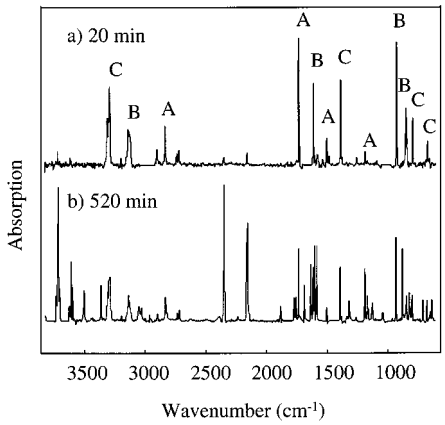

Figure 1. IR spectra of product bands of CH_3ONO_2 after 266 nm photolysis: (a) obtained after 20 min of photolysis; (b) obtained after 520 min of photolysis. The CH_3ONO_2 bands have been subtracted from the spectra.

HONO, HCOOH, and NO. The vibrational frequencies of all of these species are well-known, and the products were easily identified. All of the bands associated with these secondary photolysis products exhibit a noticeable induction period at the beginning of the photolysis period, as illustrated in Figure 3.

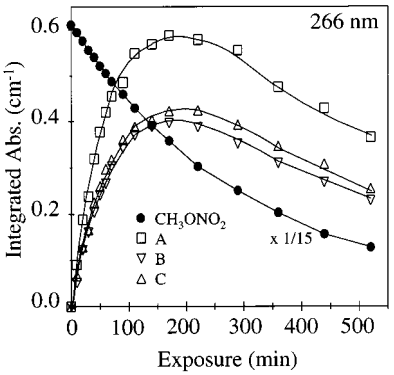

Figure 2. Kinetic behavior of the intensities of band sets A (represented by 1725.8 cm^{-1}), B (represented by 1605/1603 cm^{-1}), C (represented by 1381.6 cm^{-1}), and CH_3ONO_2 (represented by 1654 cm^{-1}) during 266 nm photolysis. For clarity of presentation, the intensity of the CH_3ONO_2 band has been multiplied by $^1/_{15}$.

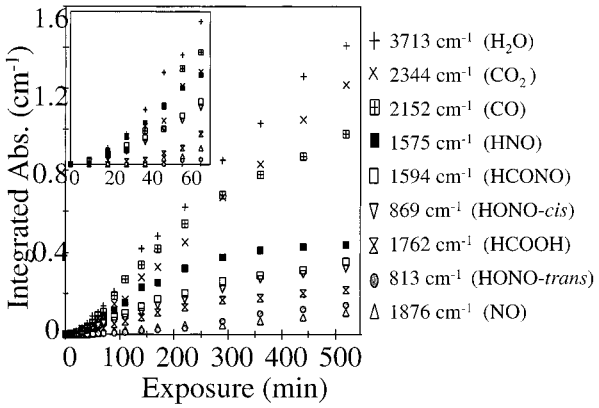

Figure 3. Kinetic behavior of the intensities of some high-order reaction products under 266 nm photolysis.

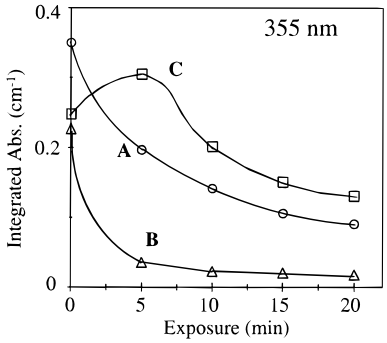

Figure 4. Kinetic behavior of the intensities of band sets A, B, and C (represented by bands observed at 1725.8, 1605/1603, and 1381.6 cm^{-1}, respectively) during 355 nm photolysis. The sample was subjected to 266 nm photolysis for 520 min prior to 355 nm irradiation.

That is to say, the rates of production of these species at $t = 0$ is essentially zero.

The infrared bands of the initial products can be ascribed to three different species, which we have labeled **A**, **B**, and **C**, on the basis of differences in their kinetic behavior upon secondary photolysis at 355 nm (Figure 4). The bands associated with initial product **A** can be readily assigned to formaldehyde, on the basis of its strong characteristic C=O stretching frequency at 1725.8 cm^{-1} for H_2CO (or 1679.9 cm^{-1} for D_2CO). Matrix-isolated H_2CO (D_2CO) has a characteristic C=O stretching frequency[11] at 1742 (1697) cm^{-1}. However, we expect that a red shift should occur when the molecule exists as a van der Waals complex with the partner photoproduct. For example,[10,11]

the C═O stretching frequency of the complex $CH_2O{\cdot}HNO$ ($CD_2O{\cdot}DNO$) is red-shifted relative to that of the isolated molecule by about 16 (12) cm^{-1}. Therefore, the 1725.8 (1679.9) cm^{-1} band observed in this experiment is assigned to a complex, one partner of which is formaldehyde. Other characteristic bands of formaldehyde were also observed and are listed in Tables 1 and 2.

The infrared bands associated with initial product **B** are assigned to hydrogen nitryl (C_{2v}-HNO_2) on the basis of a recent IR assignment of this structure by Koch and Sodeau.[19] They generated this species by 248 nm photodissociation of nitric acid isolated in an argon matrix. The band positions and relative intensities of set B in our experiment are in good agreement with their data, except for modest discrepancies in the positions of the nitrogen out-of-plane bending mode and NO_2 bending mode. The most likely reason for these discrepancies is that the hydrogen nitryl in their experiment was formed in close proximity to an oxygen atom, whereas in our experiment the partner product was a formaldehyde molecule.

On the basis of the assignments of species **A** and **B** from previous argon matrix studies, it is safe to conclude that one of the photodissociation channels of methyl nitrate is generation of H_2CO and hydrogen nitryl:

$$CH_3ONO_2 + h\nu\ (266\ nm) \rightarrow H_2CO + HNO_2\ (\text{hydrogen nitryl}) \quad (1)$$

There is no ready assignment for bands associated with initial product **C**. Because these bands all appear to belong to a single species and because the number and positions of the bands are inconsistent with any known isomer of methyl nitrate, we postulated that the two reaction channels likely had one product in common. Therefore, it became necessary to determine the quantum yield for formation of H_2CO.

We began by measuring the integrated infrared absorption coefficient of the antisymmetric stretch mode of the nitro group of CH_3ONO_2 at 1654 cm^{-1} and the C═O stretching mode of H_2CO at 1726 cm^{-1} by depositing known quantities of these stable species in argon. The method for determining the absolute quantity of each molecule in the argon matrix has been described previously.[9] The integrated absorption coefficients for CH_3ONO_2 and CH_2O are 150 and 28 km/mol (base e), respectively.

On the basis of five different 266 nm photolysis experiments on samples of CH_3ONO_2/Ar in the concentration range 1:1000 to 1:5000, we found that, at the initial stage of photolysis, destruction of one CH_3ONO_2 molecule corresponds to generation of 1.07 ± 0.16 H_2CO molecules. This result shows that H_2CO is always produced as an initial photolysis product and that products **B** and **C** must be different isomers of HNO_2 that are formed in parallel competing reaction channels.

A control experiment was performed to rule out the possibility that oxygen contamination might be contributing to production of the unidentified product **C**. Oxygen was deliberately introduced into a sample (CH_3ONO_2:O_2:Ar = 1:20:1500), and photolysis of this sample at 266 nm gave initial products for which the band positions and intensities were essentially unchanged from those of the experiments without added oxygen. It was judged unlikely that any other chemically active contaminant could have been introduced without noticing it in the infrared spectra obtained prior to photolysis.

Secondary or higher order products (shown in Tables 1 and 2 and Figure 3) are HONO (both trans and cis), HNO, CO, CO_2, NO, HCOOH,[20] H_2O, and tentatively assigned HCONO. It is important to note that HONO is not an initial product, judged from its kinetic behavior shown in Figure 3.

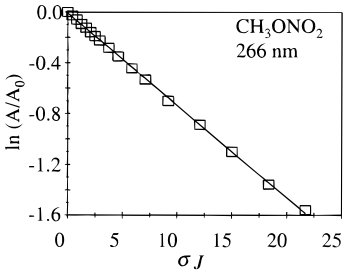

Figure 5. Plot of $\ln(A/A_0)$ vs σJ (dimensionless product of the methyl nitrate absorption cross section and the cumulative laser fluence) for determination of the photodestruction quantum yield Φ of methyl nitrate from eq 2.

For completeness, we determined the overall quantum yield for photodestruction of CH_3ONO_2 at 266 nm. This was accomplished by recording the integrated absorption intensity, A, of the nitro stretching band of methyl nitrate at 1654 cm^{-1} as a function of cumulative laser fluence, J (photons/cm^2). For optically thin samples, the quantum yield can be found from the relationship

$$\ln\left(\frac{A}{A_0}\right) = -\Phi\sigma J \quad (2)$$

where Φ is the quantum yield and σ is the 266 nm absorption cross section of CH_3ONO_2. The absorptivity of CH_3ONO_2 at 266 nm is too small to be measured directly in the argon matrix, so it was estimated from the UV absorbance of neat methyl nitrate, which was measured to be $(0.023 \pm 0.0016)/\mu$m (base 10) at 266 nm. The density of methyl nitrate is 1.15 g/cm^3, giving a molecular absorption cross section of 5.9×10^{-20} cm^2 (base e). A plot of $\ln(A/A_0)$ was found to be linear in laser fluence J, as shown in Figure 5. The slope of this plot yields an estimated quantum yield Φ for photodestruction of methyl nitrate to be 0.069 ± 0.014 at 266 nm, on the basis of an average of five experiments.

Quantum Chemical Calculations

To aid the identification of the initial product **C**, whose infrared bands have been quantified and tabulated in Tables 1 and 2, we performed ab initio quantum mechanical calculations on isomers having the empirical formula HNO_2. The five isomers of nitrous acid are shown as follows:

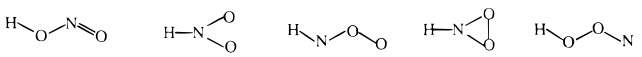

Both cis and trans forms of nitrous acid (isomer **1**) are well-known[21−24] and were determined to be secondary photolysis products in our experiments. Hydrogen nitryl (isomer **2**) was reported by Koch and Sodeau,[19] and we have assigned the product bands labeled B to this structure (vide supra). To our knowledge, isomers **3**−**5** have not been observed experimentally nor have their vibrational frequencies been calculated theoretically. The potential energies of the five isomers have been

(19) Koch, T. G.; Sodeau, J. R. *J. Phys. Chem.* **1995**, *99*, 10824.
(20) Redington, R. L. *J. Mol. Spectrosc.* **1977**, *65*, 171.
(21) John, L. H.; Badger, R. M. *J. Chem. Phys.* **1951**, *19*, 1599.
(22) McGraw, G. E.; Bernitt, D. L.; Hisatsane, I. C. *J. Chem. Phys.* **1966**, *45*, 1392.
(23) McDonald, P. A.; Shirk, J. S. *J. Chem. Phys.* **1982**, *77*, 2355.
(24) Hall, R. J.; Pimentel, G. C. *J. Chem. Phys.* **1963**, *38*, 1889.

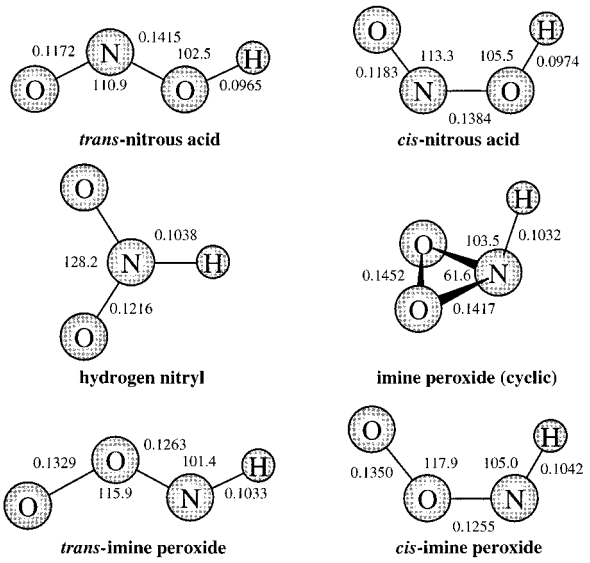

Figure 6. Optimized geometries for the HNO_2 isomers at the QCISD/6-311++G** level of theory.

theoretically studied by Fueno et al.[25] whose calculations showed that the energies increase in the order **1**−**2**−**5**−**3**−**4**. They also proposed that imine peroxide, isomer **3**, might be formed by reaction of ground-state NH with oxygen. Our calculations of the energies, structures, and vibrational frequencies of the HNO_2 isomers were undertaken with the intention of identifying product bands labeled C as being due to one of the isomers **3**−**5**.

Quantum chemical calculations were performed on all five isomers of nitrous acid (isomer **1**) employing analytical gradients with polarized split-valence basis sets (6-311++G**) at three sophisticated ab initio levels of theory, including the MP2 (full) level (meaning all electrons were included in the correlation calculations), the nonlocal density functional B3LYP level of theory, and the quadratic configuration including singles and doubles with approximate triples QCISD(T) method. All of these calculations were carried out with the Gaussian 94 program.[31] The calculated optimized geometries are shown in Figure 6, and the calculated (unscaled) harmonic frequencies are collected in Tables 3−6 for isomers **1**−**4**.

For isomer **1**, the optimized bond lengths and valence angles are in excellent agreement with the experimentally known structures,[32] and our calculated harmonic frequencies shown in Table 3 for both cis and trans nitrous acid are nearly the same at all three levels of theory and agree well with the present experimental findings. These results give some idea of the quality of the vibrational frequencies that can be expected using the basis sets and electron correlation methods that we have employed.

For isomers **2** and **4**, where simple chemical formulas can be drawn and where single-configuration-based correlation methods are expected to perform well, our ab initio calculations produce nearly identical geometries among the three methods. As a result, we believe our calculated results to be reliable for isomers **1**, **2**, and **4**. However, when isomers **3** and **5** were examined, we found significant variation in the computed geometries and vibrational frequencies as the methods used to treat electron correlation varied.

Both the trans and cis (singlet) isomers of **5** were found to be minima at the MP2(full)/6-311++G** and B3LYP/6-311++G** levels of theory, with the trans configuration being more stable than the corresponding cis. However, the optimized geometries are quite different at the two levels of theory (one of the largest ranges of geometry being 0.017 nm in the O−O distance). At the QCISD/6-311++G** level of theory, the cis isomer is not predicted to be a minimum, but a first-order saddle point with an optimal O−O distance of 0.211 nm, while the trans isomer dissociates spontaneously into NO + OH (at large O−O distances, the QCI displayed convergence difficulties). The failure of the three correlation methods to agree on isomer **5** suggests that this isomer requires a multiconfigurational treatment. One aspect of the structure for which all levels of theory agree is the O−O distance. In the both cis and trans isomers, this bond length is ca. 0.2 nm, which is considerably longer than twice the covalent radius of an oxygen atom (0.074 nm).[26] Therefore, it is reasonable to characterize isomer 5 as a weakly bound complex of two radicals, HO + NO, rather than a strongly bound molecule. This result is in agreement with the MC-SCF and MRD-CI calculations performed by Fueno et al.,[25] who found that HOON is extremely unstable and that the barrier to decompose to HO + NO is negligible. We therefore conclude that unknown isomer **C** found in the current experiments cannot be the HOON isomer **5**. Thus, it remains to examine isomer **3** as a candidate for the unknown **C**.

Both trans and cis singlet isomers of **3** were found to be minima at the MP2(full)/6-311++G**, B3LYP/6-311++G**, and QCISD/6-311++G+** levels of theory, with the cis configuration being more stable than the corresponding trans. However, the calculated optimized geometries and harmonic frequencies again are different (although the differences are less pronounced than those for isomer **5**) among the various levels of theory, again suggesting that structure **3** has appreciable multiconfigurational character in its wave function. To further consider the multiconfigurational nature of isomer **3**'s electronic state, we performed CASSCF(4,4)/6-31G**, CASSCF(6,6)/6-31G**, and CASSCF(8,8)/6-31G** calculations for both isomers of **3**. We found the optimized geometries and harmonic frequencies to vary considerably among the CASSCF(4,4)/6-31G**, CASSCF(6,6)/6-31G**, and CASSCF(8,8)/6-31G** data sets and to differ somewhat from those found at the QCISD/6-311++G** level. QCISD theory is expected to perform reasonably well when multiconfigurational character is not extreme which is certainly the case for isomer **3**, where we found the Hartree−Fock configurations to dominate ($C_{HF} = 0.9014$ for the trans isomer and $C_{HF} = 0.9077$ for the cis isomer) among the 1764 configurations in the CASSCF(8,8) expansions. We therefore believe that our results at the QCISD/6-311++G** level of theory should be reliable.

(25) Fueno, T.; Yokoyama, K.; Takane, S. *Theor. Chim. Acta* **1992**, *82*, 299.
(26) Benson, S. W. *Thermochemical Kinetics*; Wiley-Interscience: New York, 1976; p 302.
(27) Ho, P.; Bamford, D. J.; Buss, R. L.; Lee, Y. T. Moore, C. B. *J. Chem. Phys.* **1982**, *76*, 3630.
(28) Vasudev, R.; Zare, R. Z.; Dixon, R. *J. Chem. Phys.* **1983**, *96*, 399.
(29) Hido, O. In *Photochemistry of Small Molecules*; John Wiley & Sons Ltd.: New York, 1978; p 355.
(30) Gardiner, W. C., Jr. In *Combustion Chemistry*; Springer-Verlag: New York, 1984; p 167.
(31) Frisch, M. J.; Trucks, G. W.; Schlegel, H. B.; Gill, P. M. W.; Johnson, B. G.; Robb, M. A.; Cheeseman, J. R.; Keith, T. A.; Peterson, G. A.; Montgomery, J. A.; Raghavachari, K.; Al-Laham, M. A.; Zakrzewski, V. G.; Ortiz, J. V.; Foresman, J. B.; Cioslowski, J.; Stefanov, B. B.; Nanayakkara, A.; Challacombe, M.; Peng, C. Y.; Ayala, P. Y.; Chen, W.; Wong, M. W.; Anders, J. L.; Replogle, E. S.; Gomperts, R.; Martin, R. L.; Fox, D. J.; Binkley, J. S.; DeFrees, D. J.; Baker, J.; Stewart, J. J. P.; Head-Gordon, M.; Gonzalez, C.; Pople J. A. *Gaussian 94*, Revision A.1; Gaussian Inc.: Pittsburgh, PA, 1995).
(32) Fennigan, D. J.; Cox, A. P.; Brittain, A. H.; Smith, J. G. *J. Chem. Soc., Faraday Trans. 2* **1972**, *68*, 548.

Table 3. Vibrational Frequencies (cm^{-1}) of Isomer **1**, HONO (Nitrous Acid)

HONO/DONO-*trans* node	ref 21	ref 22	ref 23	ref 24	this expt	this calcn[a] (singlet)
$\nu_1(a')$	3590		3512	3558/2620	3498/2334	3838/2795
$\nu_2(a')$	1696	1699	1635	1684/1682	1680/1671	1781/1773
$\nu_3(a')$	1260	1265	1421	1298/1030	1310/1037	1342/1069
$\nu_4(a')$	794	791	801	815/769	813/...	858/802
$\nu_5(a')$		593	702	625/618	628?/636	658/645
$\nu_6(a'')$				583/444		543/410
HONO/DONO-*cis* node	ref 21	ref 22	ref 23	ref 24	this expt	this calcn[a] (singlet)
$\nu_1(a')$	3426			3410/2518	3360/2214	3688/2683
$\nu_2(a')$		1640	1611	1633/1612	1625/- - -	1724/1711
$\nu_3(a')$	1292	1261			.../992?	1361/1115
$\nu_4(a')$	856	853	857	865/828	868/...	920/889
$\nu_5(a')$		608	721		628?/618	664/607
$\nu_6(a'')$				658/522		665/508

[a] At the QCISD/6-311+G* level of theory.

Table 4. Vibrational Frequencies (cm^{-1}) of Isomer **2**, HNO_2 (Hydrogen Nitryl)

HNO_2/DNO_2 (cm^{-1})	ref 19	this expt (product **B**)	this calcn[a] (singlet)
$\nu_1(a_1)$	3289/2437	3137/2315	3278/2403
$\nu_2(a_1)$	1376/...	1372/...	1418/1396
$\nu_3(a_1)$	792/789	838/834	800/792
$\nu_4(b_1)$	1016/890	924/896	1078/911
$\nu_5(b_2)$	1600/1595	1605/1579	1665/1654
$\nu_6(b_2)$		.../1113	1561/1148

[a] At the QCISD/6-311+G* level of theory.

Table 5. Vibrational Frequencies (cm^{-1}) of Isomer **4**, HNO_2 (Cyclic Form)

HNO_2/DNO_2 (cyclic) node	this calculation[a] (singlet)
$\nu_1(a')$	3352/2453
$\nu_2(a')$	1463/1202
$\nu_3(a')$	1203/1087
$\nu_4(a')$	823/822
$\nu_5(a'')$	1259/938
$\nu_6(a'')$	812/812

[a] At the QCISD/6-311+G* level of theory.

Table 6. IR Absorption Frequencies (cm^{-1}) of Isomer **3**, HNOO (Imine Peroxide)

	this calcn[a]		
mode	*trans*-HNOO/ DNOO	*cis*-HNOO/ DNOO	possible assignt of IR absorption of set C
$\nu_1(a')$	3377/2469	3270/2387	3287/2443
$\nu_2(a')$	1540/1391	1498/1429	(notobs.)
$\nu_3(a')$	1391/1199	1425/1177	1382/1081
$\nu_4(a')$	841/816	899/894	843/823
$\nu_5(a')$	660/635	632/577	670/659 or 670/588
$\nu_6(a'')$	794/599	875/699	791/588 or 791/659

[a] At the QCISD/6-311+G* level of theory.

At our highest QCISD(T)/6-311++G(2df,2pd) level of theory, the cis configuration of isomer **3** was found to be more stable by 13.0 kJ/mol than the trans configuration. We attempted to calculate the barrier connecting the trans and cis configurations at the QCISD/6-311++G** level of theory. However, when the HNOO dihedral angle approached 60°, we met QCI convergence problems, and therefore, we were unable determine the value of the trans−cis isomerization barrier, although we can say that the barrier is at least 57 kJ/mol, the last geometry where convergence was realized.

Discussion

1. Identification of Product C. Good agreement was found between the experimentally observed and readily identified infrared band positions and the calculated vibrational frequencies for isomer **1**, nitrous acid (Table 3), and for isomer **2**, hydrogen nitryl (Table 4). This gave us confidence that the quality of the calculations was sufficient for assigning the structure of product **C** and that any perturbations in frequencies due to the argon matrix environment and the presence of a formaldehyde reaction product would not be so severe as to make the assignment ambiguous.

The calculated vibrational frequencies of isomer **4**, HNO_2 (cyclic form), and of isomer **3**, HNOO, are listed in Tables 5 and 6, respectively. We found that the set of product bands C could not be matched to the calculated vibrational frequencies of isomer **4**, HNO_2 (cyclic form), but can be fit well to either the trans or cis forms of isomer **3**, HNOO, although the agreement with the trans form is somewhat better. Unfortunately, we were unable to positively identify any bands in the experiments corresponding to the ν_2 vibration of HNOO (see Table 6). This is possibly due to a weak absorption cross section for this vibrational mode. We should stress that the calculated frequencies are for isolated gas-phase HNOO, whereas the observed frequency is for HNOO complexed by a cage partner H_2CO molecule. The NH stretching frequency of $CH_2O{\cdot}HNO$ is blue-shifted[11] relative to that of HNO by 60−90 cm^{-1}. Because the calculations do not include effects of anharmonicity or complexation, the calculated NH frequency could be overestimated by 100 cm^{-1}. Therefore, the agreement between calculation and experiment is quite reasonable. As mentioned earlier, our calculations showed that cis form is more stable (about 13 kJ/mol below trans), and the barrier between cis and trans is very high (>57 kJ/mol). The high barrier to interconversion means that any trans isomer will remain trans at the temperatures of the argon matrix experiments. It is therefore somewhat surprising that we observe only one of the two isomers. Unfortunately, there is not enough difference in the patterns of the calculated vibrational frequencies to determine with certainty which of the two conformers is observed.

2. Initial Photodissociation Channels of Methyl Nitrate under 266 nm Radiation. On the basis of the infrared band assignments and the measured quantum yield of CH_2O, we have demonstrated that photodissociation of methyl nitrate in an argon matrix proceeds by two parallel channels, each of which forms a thermodynamically unstable isomer of nitrous acid:

$$CH_3ONO_2 + h\nu\ (266\ nm) \rightarrow H_2CO + HNO_2\ (\text{hydrogen nitryl}) \quad (1)$$

$$CH_3ONO_2 + h\nu\ (266\ nm) \rightarrow H_2CO + HNOO\ (\text{imine peroxide}) \quad (3)$$

In principle, it should be possible to determine the branching ratio between the two channels by comparing the integrated band intensities of products **B** and **C** corrected for differences in the calculated absorption coefficients (Tables 4 and 6). However, we found that the uncertainties in the calculated band intensities (as judged by comparison of experimental and calculated intensity distributions for each isomer, nitrous acid, hydrogen nitryl, and imine peroxide) were too large to make a quantitative evaluation of the branching ratio. But, on a qualitative basis, it appears that the contributions of the two channels (reactions 1 and 2) are comparable.

HONO (both trans and cis) is not an initial product of 266 nm photodissociation of methyl nitrate (from their dynamic behavior shown in Figure 3). It is likely the secondary photochemical product of HNO_2 (hydrogen nitryl) or HNOO.

Other products might be explained on the basis of the two initial channels. Photodissociation of H_2CO produces H, HCO, and CO.[27] Photodissociation of HONO results in OH and NO.[28] Photodissociation of any of the HNO_2 isomers in the presence of CH_2O could lead to photooxidation of the latter to HCOOH, which is observed in this experiment. Reaction of H and NO could result in HNO, which is also an observed secondary product. Another high-order reaction product is probably HCONO, which could be formed by reaction of HCO with NO. CO_2 can be formed via oxidation of CO by OH at very low temperature.[29,30]

Conclusion

There are two initial photodissociation channels of matrix-isolated methyl nitrate under 266 nm radiation. One is $H_2CO + HNO_2$ (hydrogen nitryl), and the other is H_2CO + HNOO (imine peroxide). Quantum chemical calculations of the structures and vibrational frequencies of five isomers of nitrous acid are presented. The ab initio frequencies were used to assign experimentally observed compound **C** to HNOO (imine peroxide). This is the first report of the formation, detection, characterization, and vibrational spectrum of imine peroxide.

Acknowledgment. The experimental part of this research was supported by the Office of Naval Research, Program Officer Dr. Richard S. Miller, under Contract N-00014-95-1339, and the theoretical part was supported by NSF Grant CHE-9618904.

JA9824223